

# Development of an Innovative Inspection Tool for Superheater Tubes in Fossil Energy Power Plants

Caique Lara, Julie Villamil, Anthony Abrahao, Aparna Aravelli,  
Guilherme Daldegan, Sharif Sarker, Daniel Martinez\*, Dwayne McDaniel

Mechanical and Materials Engineering  
Applied Research Center  
Florida International University

\*George W. Woodruff School of  
Mechanical Engineering  
Georgia Institute of Technology

## 1 Abstract

Fossil fuel power plants are complex systems containing multiple components that require periodic health monitoring. Failures in these systems can lead to increased down time for the plant, reduction of power and significant cost for repairs. Inspections of the plant's super-heater tubes are typically manual, laborious, and extremely time consuming. This is due to their small diameter size (between 1.3 and 7.6 cm) and the coiled structure of the tubing. In addition, the tubes are often stacked close to each other, limiting access for external inspection. This article presents the development and testing of an electrically powered pipe crawler that can navigate inside 5 cm diameter tubes and provide an assessment of their health. The crawler utilizes peristaltic motion within the tubes via interconnected modules for gripping and extending. The modular nature of the system allows it to traverse through straight sections and multiple 90° and 180° bends. Additional modules in the system include an ultrasonic sensor for tube thickness measurements, as well as environmental sensors, a LiDAR and camera. These modules utilize a gear system that allows for 360° rotation and provides a means to inspect the entire internal circumference of the tubes.

**Keywords:** internal pipe crawler, robotics, inspection, superheater tubes

## 2 Introduction

The power generation of a superheater powerplant relies on burning coal to boil water and convert it to steam. The superheated steam, produced in the combustion chamber, is directed to the turbines of the plant to generate electricity by converting the kinetic energy of the fluid into electrical energy. The combustion chamber contains numerous pipes, typically found in a coiled structure, that operate at temperatures up to 540°C and pressures between 10 to 1000 bar. In addition, the tubes range from 1.3 to 7.6 cm in diameter [1]. These tubes are located in the hottest region of the steam generator and can fail if maintenance and inspections are conducted infrequently. Prolonged operation can result in the rupture of critical components, stemming from plastic deformation and surface oxidation [2].

To avoid failure, an inspection of the superheater tubes should be done periodically. Typically, these inspections are conducted externally, and are often manual and time-consuming. They are also challenging, as some areas are difficult to reach and the environment can be dangerous for humans. Recently, robotic inspections have seen an increase in utilization as an alternative to human-based examinations [3]. One approach using robotic inspections is to conduct the evaluation on the external surface of the pipes or tubes [4]. These devices [5–10] crawl on the external surface of the tubes using different adhesion mechanisms including suction [8], thrust propellers, and magnets [9]. These systems can detect pinholes, cracks, and thickness reduction due to erosion and corrosion using sensors such as electromagnetic acoustic transducer [10] and other non destructive tools.

Although some of the technical issues with external systems have been addressed, there are still some challenges that need to be investigated. This includes the potential difficulty of navigating on pipes with limited external access. An example includes boiler superheater tubes that are often stacked and don't allow for the external inspection of the tubes inside the combustion chamber. Internal inspection systems offer an alternative to the more conventional external approach. These systems do not have issues with the external constraints, but have their own challenges due to the reduced availability of space. They also can require the system to be shut down prior to the inspection. Several designs and concepts for in-pipe inspection systems have been discussed in the literature [11–22]. These systems perform a variety of tasks including internal cleaning of ducts [17], measurement of surface thickness, mapping of tubes, and visual inspection [18].

One of the significant challenges for internal crawler systems is the ability to generate traction within the limited space of the tubes. Earthworm type robots [19, 20] offer larger traction output, but require a number of degrees-of-freedom. Wheeled [21] and treaded [22] systems offer simpler designs but generate less traction. The compromise between maneuverability and design simplicity is a major challenge in developing a robotic inspection system. However, there is little research that has been conducted on the development of internal crawlers for superheater tubes and small diameter pipes, in general. This is likely due to the limited space available and the coiled nature of the tubes.

In this article, a novel robotic inspection tool is presented that can navigate through small diameter pipes and provide information on the structural integrity of tubes typically found in powerplant superheaters. The

system consists of a tethered pipe crawler that can navigate through the coiled tubes, with 180° bends and diameters as small as 5 cm. The primary crawler will contain modules that house inspection sensors including a LiDAR, environmental sensors, cameras, and an ultrasonic sensor for measuring tube thickness. Multiple auxiliary crawlers will also be utilized for load distribution of the tether as the system navigates through the multiple bends and straight sections. A schematic of the concept is shown in Figure 1.

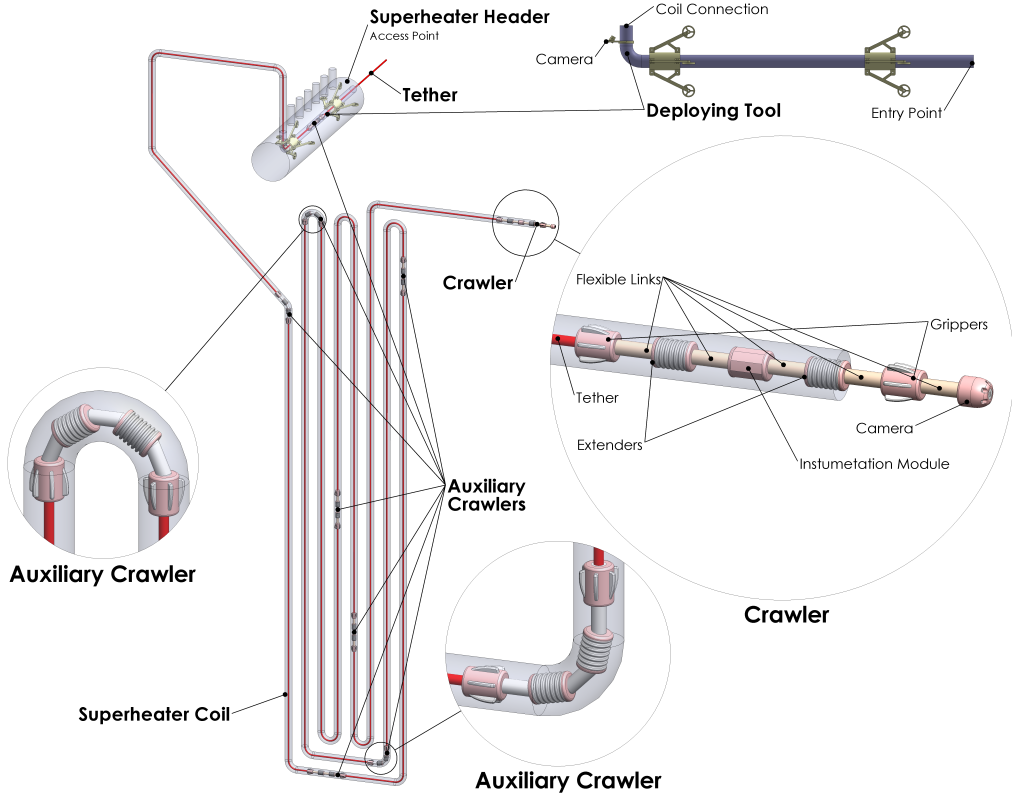


Figure 1: Conceptual design of the crawler inspection system

### 3 Robotic Crawler

#### 3.1 System Description

Movement of the crawler is generated using a set of gripper and extender modules that propel the crawler forward using peristaltic motion, similar to earthworms that travel by contracting their body segments sequentially. Each module holds a linear actuator consisting of a rotating lead screw and nut. The basic design is composed of five modules: two grippers, one at the front and one near the rear of the system, two extenders, between the grippers and one electronics module. The modules are connected via a flexible cable that has the strength to handle the push/pull loads and is also flexible enough to allow for significant rotation between the modules.

Each gripper contains linkage arms that push small pads radially outward and engage the inner pipe wall. The radial symmetry of the design allows for three sets of linkage arms and gripper pads. These linkages are driven by a mechanism attached to the nut of the rotating lead screw. Similarly, the extenders utilize a nut at the center of the module which expands and contracts. Two electric motors on the sides of the module utilize a gearbox to power the lead screw.

The selection of actuators was critical to the design of the crawler. The choice of electric linear actuators versus pneumatic actuators involved consideration of several factors. Reliance on compressed air throughout the crawler posed a challenge in the tether design management. Additionally, electric motors are much smaller and required thinner wiring than the pneumatic motors. It should be noted that there was a clear trade-off between reducing the module's overall dimensions versus simplifying the controls of the system. Pneumatic actuators provide a much simpler method of producing the linear motion.

This challenge was addressed in developing the electronics and communication system for the crawler. A module has been incorporated into the system that houses the major electronic components. This includes the embedded microcontroller, voltage regulator, current sensors, and motor controllers that are mounted onto printed circuit boards. The electronics module was added to the rear end of the system and controls the movement of each gripper and extender. Figure 2 shows a prototype of the base crawler system with the five modules.



Figure 2: Prototype of the base robotic crawler

### 3.2 Simulation Model

The development of the crawler significantly depended on the coil geometry. In an initial geometric analysis, efforts were made to design the system to be capable of navigating through 5 cm radius bends. This led to the modules having a maximum diameter of 3.5 cm and a maximum length of 7 cm.

To improve the design of the peristaltic crawler and set the framework to evaluate the controls of the system, a high-fidelity model is being developed. Figure 3 shows a detailed schematic of the gripper and extender modules and includes key components and dimensions. The gripper module consists of a total of 31 bodies and uses 14 joints to incorporate the constraints needed to generate the required motion. In addition, 16 constraints are used to implement limitations on the motion. The bodies include two end caps that can be used to mount the flexible connecting cable between the modules, a lead screw, a lead nut and a helical spring. Additionally, there are 9 links connecting the spring and the bottom end caps that support the gripper pad with a revolute joint. This joint provides the constraints so that the pads can contact the internal pipe surface, regardless of the orientation of the linkage. A micro-gear motor is used to rotate the lead screw and expand the linkages that mate the pads with the pipe surface. Similarly, the extender consists of 22 bodies and uses 8 joints to generate the motion. However, only 1 motion constraint is required which limits the module's extension distance. Two micro-gear motors are used in the extender to provide the necessary torque on the lead screw that extends the top of the module. The stroke length for each module is approximately 2.58 cm, resulting in 5.16 cm of displacement for each cycle of the crawler.

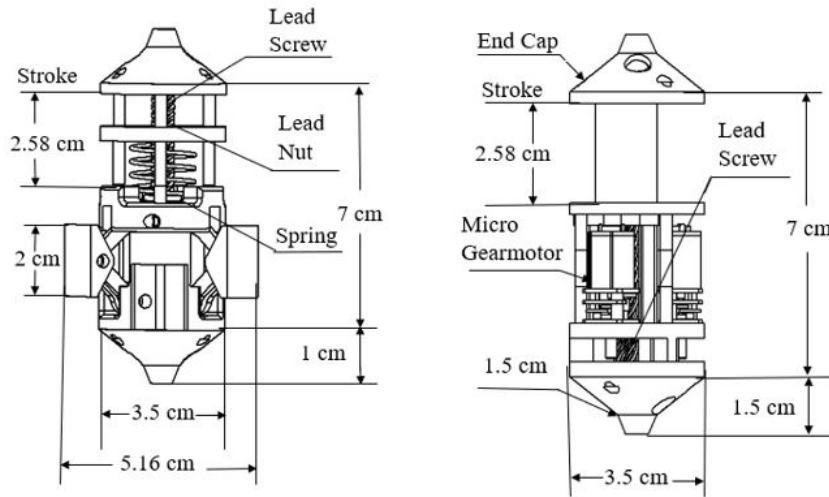


Figure 3: Schematic of the gripper and extender modules

### 3.3 Motion Analysis

To generate peristaltic motion of the crawler, the gripper in the rear extends and fixes its position within the tube while the other modules are collapsed. With the rear gripper position fixed, the two extenders simultaneously extend, moving the front gripper forward 5.16 cm. The front gripper then extends, fixing its position within the tube, and the rear gripper collapses. The two extenders then retract pulling the rear gripper forward 5.16 cm. The cycle generates 5.16 cm of motion for the crawler and is repeated continuously until the crawler reaches its destination.

In addition, a simplified force analysis of a single gripper and extender in a static state was conducted. The gripper must be capable of generating a friction force greater than the drag force generated from the tether. If the friction force is lower than the drag force, the gripper will slip backwards. Similarly, when the extender is retracting, it must be capable of overcoming the tether load, or there would be no motion generated.

A simulation of the gripper and extender was created using motion simulation package. The analysis included extending one gripper that was resting on the bottom of a 5 cm tube. A motor drives the lead screw which extends the gripper arms until the three pads reach the tube inner wall, as shown in Figure 4.

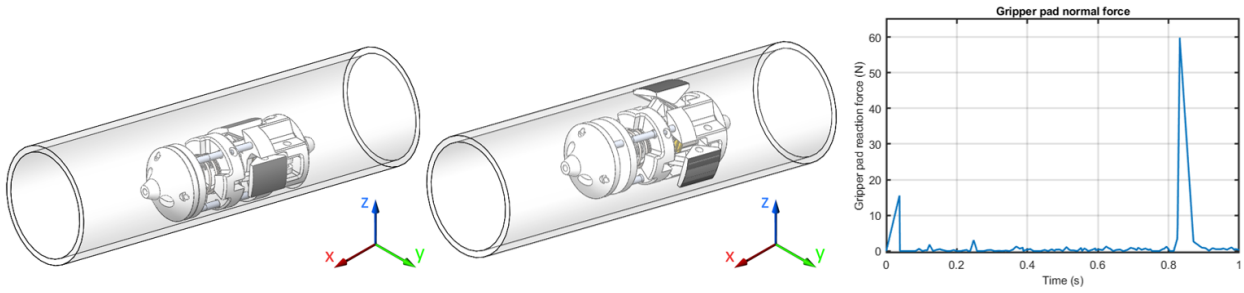


Figure 4: Motion analysis of the gripper

The normal force produced from the simulation is also shown in Figure 4. A peak force of approximately 60 N was obtained for one gripper. The result also shows smaller peaks in the normal force as the linkage arms extend. These peaks were due to the weight of the gripper on the lower arm. The friction force generated by the gripper is dependent on the normal force and the coefficient of friction between the pad and tube wall. For this analysis, a coefficient of friction of 0.6 was used for the interface between the rubber pad and steel tube surface. This was experimentally determined in accordance with ASTM D1894 [23] and is in agreement with standard values provided in the literature. This provides a maximum static friction force of 36 N per pad. With the three pads, this results in a simulated force of 108 N.

Additional data from the simulation with the gripper shows the axial motion of the lead screw, the radial displacement of the arm linkage, and the radial displacement of the gripper pad (Figure 5). The simulation was conducted from the closed position to the extended position. As the nut is moved forward, the angle of the linkages change and moves the gripper pad toward the inner pipe.

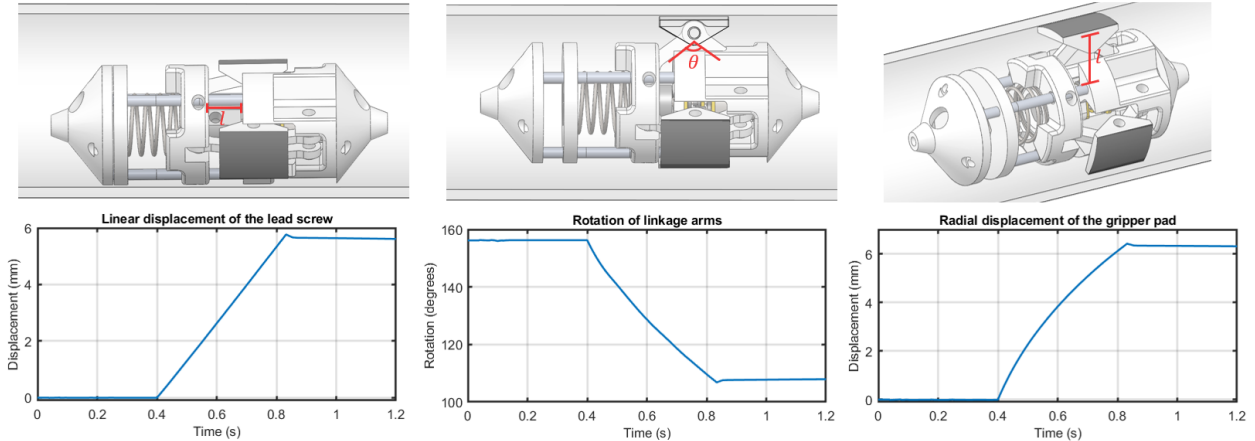


Figure 5: Gripper component motion

A simulation was also conducted of the extender module. Similar to the gripper, a motor drives a lead screw, causing the lead nut to extend toward the module's end cap. The maximum extension of the module is 2.58 cm. Both of the front and back gripper modules will be connected to the extender modules via short flexible wires.

## 4 Inspection Modules

The purpose of the crawler is to provide information regarding the structural integrity of key pipeline components in fossil energy power plants. Although cameras will be incorporated into the front and rear modules, additional modules have been developed to house inspection sensors and are described in the following subsections.

### 4.1 Ultrasonic Transducer Module

One of the sensors that will be used to assess the integrity of the tubes is an ultrasonic transducer (UT) sensor. A module has been developed that will house and deploy the UT sensor for tube thickness measurements. The module will be used to measure the thickness at any location within the tube. To move the UT sensor radially to the inner surface, a deployment mechanism was developed. The mechanism utilizes two micro-motors connected to a gearbox and a lead screw. The lead nut is attached to a housing for the UT sensor and translates along the lead screw, converting the rotary motion from the motors to a linear motion for the sensor.

To aid in obtaining thickness measurements at different circumferential locations, a spur gear system was added. A stationary spur gear is mounted on the front-end of the module and acts as the output shaft. The input shaft gear, connected to a micro-motor, spins with the module. A set of bearings permits the rotation and reduces the friction between the moving parts. This mechanism provides a full 360° rotation of the modules and provides a means for the UT sensor to measure the tube thickness at any radial location. A schematic of the module highlighting the major components is showed in Figure 6.

To keep the module centered and maintain stability during the rotations, a stabilization system is included that utilizes three lever arms for support. The three arms have linkages with a pair of springs attached to each link. The springs provide a constant opposing force to a set of wheels mounted on the end of the arm. This spring force offsets gravity during the rotation of the module and establishes continuous surface contact for each of the wheels. The stabilization systems allows for accurate positioning of the sensor while obtaining wall thicknesses measurements of the tube.

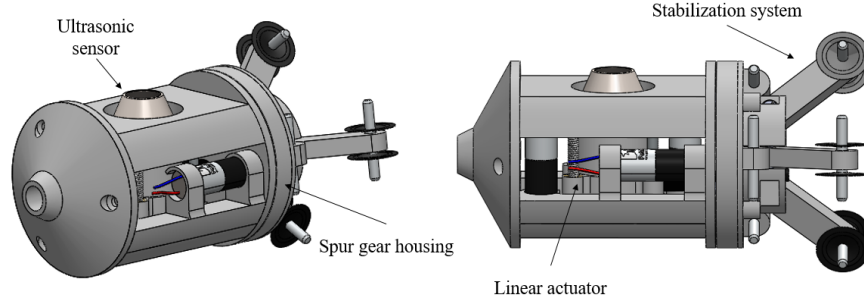


Figure 6: UT sensor module schematic

During the evaluation of different UT sensors, it was clear that even the smallest sensor head of 7 mm used in this study did not make significant contact with the curved internal tube surface. The small gap between the two surfaces, as shown in Figure 7, led to an offset in the thickness measurements of the 5 cm diameter tube. To evaluate the consistency of the thickness offset, a stepped steel tube section was machined to create gradually varying thicknesses along the length of the tube. The wall thickness decreased 0.198 mm at each step. Figure 7 also shows the machined tube and the thickness steps created. Thicknesses measurements were taken from both the inside and outside surfaces of the machined tube. Since the probe had more surface contact on the outside surface, these measurements were found to represent the actual thickness. For each thickness step, twenty measurements were obtained and averaged. The results, shown in Figure 7, were plotted with the blue line representing the measurements from the inside surface and the red line representing the measurements from the outside surface.

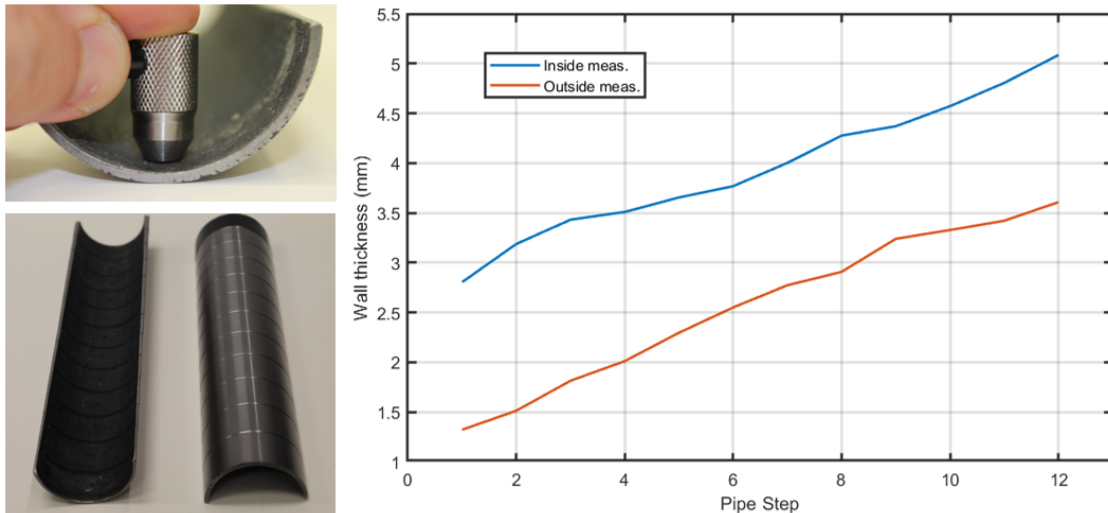


Figure 7: Thickness measurements obtained from the inside and outside surfaces of a tube with varying thicknesses

Several factors can affect the accuracy of measurements using a UT sensor: the angle of incidence, the couplant, diameter of the sensor head and the curvature of the pipe. Results from this analysis show that although the measurements taken from inside surfaces were off, the offset from the true thickness was fairly consistent and could be used to obtain reasonably accurate measurements.

## 4.2 Surface Preparation Module

The ultrasonic sensor used in the UT module requires a liquid couplant to obtain measurements. The gap between the sensor tip and the surface should be filled with a fluid to permit the ultrasonic signals to travel to and from the wall surface. Water can be used as the couplant, however, denser liquids allow for a higher refraction of the signals. Thus, a gel couplant offers a better alternative and was utilized in this system. Couplant-free ultrasonic sensors were considered for this study, however, they can require large application forces to compensate for potential gaps. Due to space limitations within the crawler, these requirements are difficult to achieve with the small electric motors currently available. In addition to the surface gap, moisture and elevated temperatures in superheater tubes increases levels of corrosion and creep in the tubes. To address these challenges, a separate module was developed for application of a gel couplant and surface-cleaning brush as shown in Figure 8.

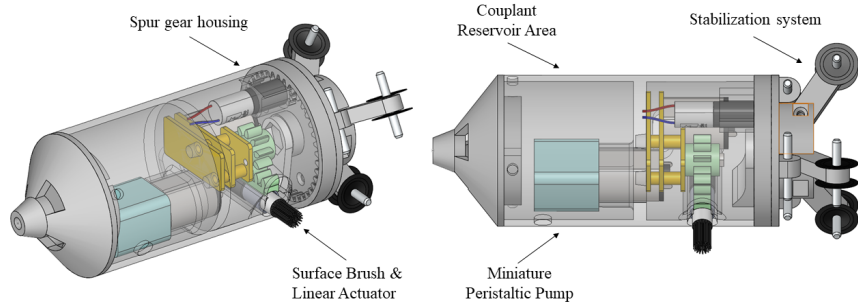


Figure 8: Surface preparation module

The design of the module includes four motors which rotates and extends a surface brush, drives a pump to apply a couplant, and rotates the module. To apply the gel couplant needed for the UT sensor, a peristaltic pump is used to transfer the gel from a reservoir to the tube inner surface. A chamber at the front of the module houses a reservoir containing the gel and the pump. Due to the available space in the module, the pump selected was based on its size, flow rate, pressure, and compatibility with the liquid.

The surface-cleaning brush is attached to a motor mounted perpendicular to the module. Radial extension of the brush and it's motor is accomplished using a rack and pinion gear. This allows the components that make up the brush to fit within the diameter of the module. The brush can then be positioned on the tube surface for cleaning when needed.

Since the UT sensor will need to obtain measurements around the circumference of the tube, this module also contains a spur gear system for rotation. This will allow the module to rotate and prepare the internal surface for measurements using the brush and couplant. Testing of the module was conducted in a clear 5-cm diameter tube to evaluate surface-brush contact and application of the gel couplant.

### 4.3 Instrumentation Module

To improve the functionality of the crawler, an instrumentation module was developed that contains a variety of sensors to evaluate the conditions within the tube. Similar to the previous modules, this module uses a carousel-type motion with a spur gear system (Figure 9). Six modular panels spin 360° concentrically about the center of the tube. Each panel design can be modified to support a different sensor.

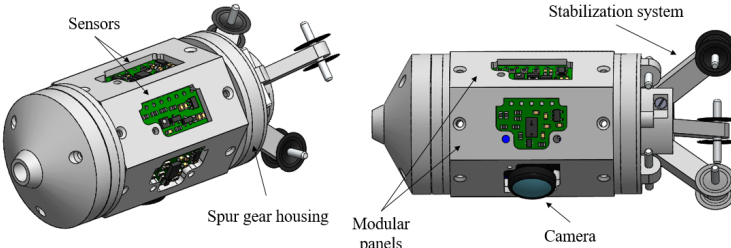


Figure 9: Schematic of the instrumentation module

The module currently includes 3 sensors for assessing the tube conditions, although there are 3 more panels available for additional sensors in the future. The three current sensors include an analog video camera, an environmental sensor for temperature and pressure measurements, and a light detecting and ranging sensor (LiDAR). The LiDAR can provide information on potential surface anomalies and defects. An inertial measurement unit is also included in the module and provides the angular position and acceleration of the crawler. An embedded microcontroller manages the communication between the sensors and the electronics module discussed in Section 3.1. Table 1 shows the specifications of the sensors currently installed in the module.

Table 1: Sensor specifications

| Sensor               | Measurement             | Range        | Resolution | Unit  | Model    |
|----------------------|-------------------------|--------------|------------|-------|----------|
| Environmental        | Temperature             | -40 – +85    | ±1         | °C    | LPS25HB  |
|                      | Pressure                | 26 – 126     | ±0.02      | kPa   |          |
| Inertial Measurement | Acceleration            | ±2 – ±16     | ±0.004     | g     | LSM6DS33 |
|                      | Angular Velocity        | ±125 – ±2000 | ±10        | °/s   |          |
| Camera               | Surface Imaging         | 640X480      | VGA        | Pixel | Generic  |
| LiDAR                | Circumferential Mapping | 10 – 60      | ±1         | mm    | VL6180X  |

## 5 Testing

The development of the crawler system started with creating general concepts and initial prototyping and proceeded with bench-scale testing and engineering-scale testing of the system. This section presents the bench-scale testing used to validate the concepts and testing of the system in a tube with multiple bends and straight sections.

### 5.1 Bench-Scale Testing

#### *Robotic Crawler*

To evaluate the pull force capability of the crawler, pull force tests were conducted on the gripper and extender modules. The grippers were found to be capable of pulling approximately 84.5 N of force and the extenders were found to generate 40 N of force. These values demonstrate that the forces obtained in the motion analysis (Section 3.3) are reasonable approximations of the actual pull forces. The pull force tests were conducted using a digital weight scale attached to the ends of the modules. The value for the gripper was found by finding the maximum pull force before the gripper pads began to slip along a steel 5 cm diameter tube. The pull force for the extender was found by clamping the module to a flat surface and allowing the linear actuator to pull the scale.

After the initial system was assembled, bench-scale tests were conducted to evaluate the crawler's ability to navigate through both straight and 180° elbow sections (Figure 10). The elbow testing was conducted in a custom built 5 cm diameter tube with a 7 cm bend radius. Although the system was designed to navigate through bends with a 5 cm radius of curvature, the smallest bend radius found in a transparent acrylic pipe was 7 cm. With this experimental setup, the crawler was easily able to navigate through the bend. The average speed of the crawler in straight sections was found to be 50 cm/min. The speed was slightly slower when navigating through the bends.

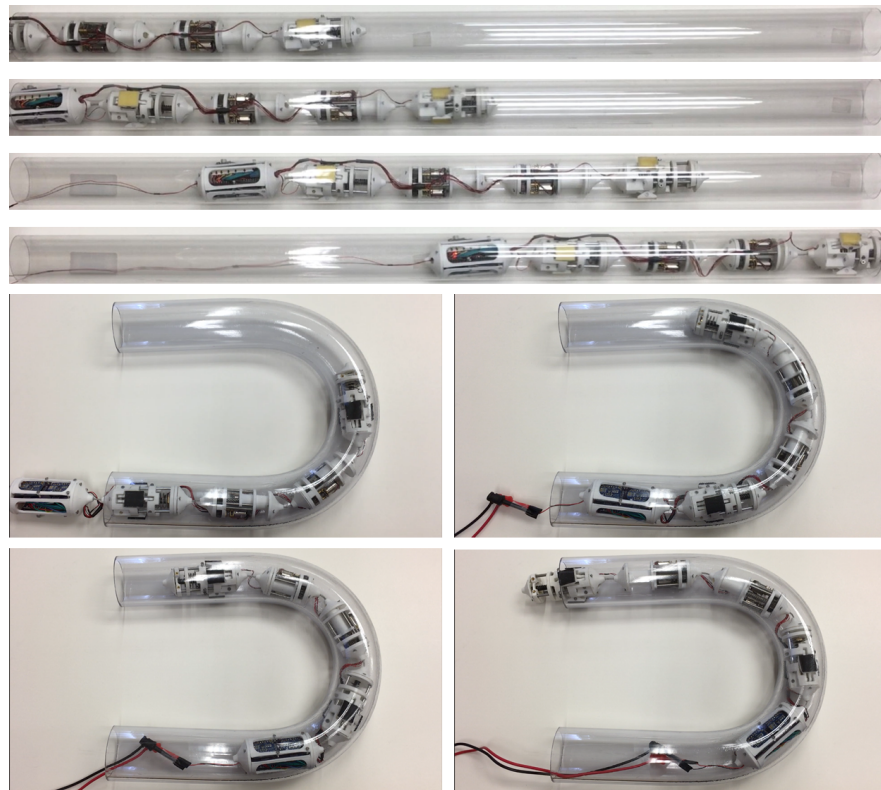


Figure 10: Robotic crawler traveling in straight tube section and plastic U-bend

#### *Ultrasonic Transducer Module*

To demonstrate the functionality of the UT module, tests were performed in a clear acrylic 5 cm diameter straight tube with a wall thickness of 1.6 mm. The UT gauge was calibrated to measure the thickness of PVC by adjusting the velocity of sound to 2390 m/s. Since the module was not integrated with the crawler for the bench-scale testing, the stabilization mechanism was adapted to be used at both ends of the module. Figure 11 shows the test performed with the module. Wall thickness was measured at three different locations around the inner circumference of the tube.



Figure 11: Measurements performed on the tube's inner surface

The circumferential rotation using the spur gear set allowed the module to obtain measurements at different locations along the inner wall of the tube. As shown in Figure 11, the measurements were consistent between 2.5 and 2.6 mm. As noted in Section 4.1, the flat sensor head does not mate perfectly with the internal tube surface due its curvature. Thus, an offset must be subtracted from the measurement to obtain a more accurate reading.

#### *Instrumentation Module*

To evaluate the laser range detection sensor in the instrumentation module, a template ring was used to simulate a 5 cm diameter surface with a variety of irregularities. During the testing, the module is positioned at the center of the template frame and rotates to scan the surrounding irregularities on the ring. Figure 12 shows the template ring and the instrumentation module positioned at the center.

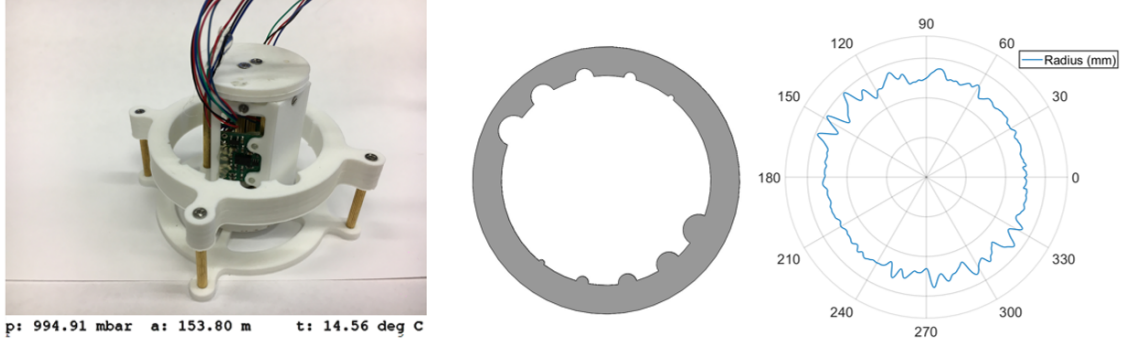


Figure 12: Instrumentation module testing

Preliminary results demonstrate the potential for the detection of anomalies in tubes and pipes using the VL6180X LiDAR sensor. Data from the environmental sensor is also shown and includes pressure (p), altitude (a), and temperature (t). It should be noted that the camera was not installed during this testing.

## 5.2 Engineering-Scale Testing

To evaluate the crawler's performance in a larger scale testbed, a mock-up similar to the superheater tubes found in fossil energy power plants was constructed. The testbed was manufactured with acrylic plastic tubes so the crawler could be observed while navigating through the straight sections and 180° elbows. As shown in Figure 13, the crawler was able to navigate through multiple straight pipe sections and bends and was only limited by the length of the tether.

An additional testbed is being constructed with metal tubes and contains sharper bends, as well as 90° elbows. This setup will not allow for visualization of the crawler, but will provide a more realistic testbed to evaluate its pull force capability.



Figure 13: Crawler navigating the superheater tube mock-up with magnified images

## 6 Conclusion and Future Work

A robotic crawler has been developed that can navigate through 5 cm diameter tubes similar to those found in fossil energy power plants. The base modules for navigation include two grippers and two extenders. The maximum pull force of the system is limited by the strength of the extenders which is 40 N. Once the drag force of the tether reaches this value, an additional crawler would need to be inserted to assist in the load distribution. Additional modules have been developed that include an electronics module, a UT sensor module, a surface preparation module, and an instrumentation module. Testing of the crawler system demonstrates its ability to navigate through multiple straight sections and 180° bends. Initial testing of the modules demonstrate the system's ability to inspect the integrity and conditions within 5 cm diameter tubes.

A number of issues will continue to be investigated in efforts to improve the performance of the system. Since the distance the crawler can navigate is limited by its pull force capability, efforts will be made to improve the extenders and grippers and reduce the drag on the system. Design modifications will include incorporation of the stabilization mechanism in the gripper and extender modules to reduce drag and improve the performance in elbows. Efforts will also continue to focus on improving the wire management by incorporating slip rings in the rotating modules.

The individual microcontrollers in each module currently utilize serial protocols for communication between the modules. Additional protocols will be evaluated including RS-485, CAN Bus, and SPI that may provide more efficient and streamlined communication. This will also establish the controls for supplying power, streaming sensor data, and analog video feedback. Data from the camera and sensors will be collected and managed using a control box that will house a user interface for live video feedback. The software that will manage both the communication protocol and the interface is currently being developed. Future engineering-scale testing will be conducted with a fully developed communication system and integration of the sensor modules.

Testing of the sensors in the instrumentation module was conducted with simple sensors that were commercially available off the shelf. Future efforts will also include improving the accuracy and resolution of the sensors by investigating alternate sensors with improved performance.

A high fidelity model will also continue to be developed. Accurate models of each module will be integrated together and provide a platform for developing a virtual environment for evaluation of the system. This will allow for the assessment of module design changes, system additions to augment the crawler's functionality, and control strategies to maximize the performance of the system. In addition, multiple crawlers will be integrated to maximize the distance the system can navigate.

## 7 Acknowledgments

The authors would like to thank DOE-NETL for their financial support. This research effort was funded under Award Number DE-FE0031651.

## 8 References

- <sup>1</sup>F. Dehnavi, A. Eslami, and F. Ashrafizadeh, “A case study on failure of superheater tubes in an industrial power plant”, *Engineering Failure Analysis* **80**, 368–377 (2017).
- <sup>2</sup>G. J. Abraham, V. Kain, and N. Kumar, “Cracking of superheater tube in a captive power plant”, *Corrosion Engineering Science and Technology* **53**, 98–104 (2018).
- <sup>3</sup>A. Nayak and S. K. Pradhan, “Design of a new in-pipe inspection robot”, *Procedia Engineering* **97**, 2081–2091 (2014).
- <sup>4</sup>S. D. Kapayeva, M. J. Bergander, A. Vakhguelt, and S. I. Khairaliyev, “Remaining life assessment for boiler tubes affected by combined effect of wall thinning and overheating”, *Journal of Vibroengineering* **19**, 5892–5907 (2017).
- <sup>5</sup>J. Shang, B. Bridge, T. Sattar, S. Mondal, and A. Brenner, “Development of a climbing robot for inspection of long weld lines”, *Industrial Robot* **35**, 217–223 (2008).
- <sup>6</sup>C. Balaguer, A. Giménez, J. M. Pastor, V. M. Padrón, and M. Abderrahim, “Climbing autonomous robot for inspection applications in 3D complex environments”, *Robotica* **18**, 287–297 (2000).
- <sup>7</sup>G. La Rosa, M. Messina, G. Muscato, and R. Sinatra, “A low-cost lightweight climbing robot for the inspection of vertical surfaces”, *Mechatronics* **12**, 71–96 (2002).
- <sup>8</sup>D. Longo and G. Muscato, “A modular approach for the design of the Alicia3 climbing robot for industrial inspection”, *Industrial Robot* **31**, 148–158 (2004).
- <sup>9</sup>M. Tavakoli, C. Viegas, L. Marques, J. N. Pires, and A. T. De Almeida, “OmniClimbers: Omni-directional magnetic wheeled climbing robots for inspection of ferromagnetic structures”, *Robotics and Autonomous Systems* **61**, 997–1007 (2013).
- <sup>10</sup>P. Sangdeok, D. J. Hee, and S. L. Zhong, “Development of mobile robot systems for automatic diagnosis of boiler tubes in fossil power plants and large size pipelines”, in *Proceedings ieee/rsj international conference on intelligent robots and systems* (2002).
- <sup>11</sup>A. Hadi, A. Hassani, K. Alipour, R. Askari Moghadam, and P. Pourakbarian Niaz, “Developing an adaptable pipe inspection robot using shape memory alloy actuators”, *Journal of Intelligent Material Systems and Structures* **31**, 632–647 (2020).
- <sup>12</sup>T. Kishi, M. Ikeuchi, and T. Nakamura, “Development of a Peristaltic Crawling Inspection Robot for Half-Inch Pipes Using Pneumatic Artificial Muscles”, *SICE Journal of Control, Measurement, and System Integration* **8**, 256–264 (2015).
- <sup>13</sup>S. Tesen, N. Saga, T. Satoh, and J. ya Nagase, “Peristaltic Crawling Robot for Use on the Ground and in Plumbing Pipes”, *CISM International Centre for Mechanical Sciences, Courses and Lectures* **544**, 267–274 (2013).
- <sup>14</sup>H. Omori, T. Nakamura, and T. Yada, “An underground explorer robot based on peristaltic crawling of earthworms”, *Industrial Robot* **36**, 358–364 (2009).
- <sup>15</sup>P. Debenest, M. Guarnieri, and S. Hirose, “PipeTron series-Robots for pipe inspection”, *Proceedings of the 3rd International Conference on Applied Robotics for the Power Industry, CARPI 2014*, 10.1109/CARPI.2014.7030052 (2015).
- <sup>16</sup>J. Y. Nagase, K. Suzumori, and N. Saga, “Development of worm-rack driven cylindrical crawler unit”, *Journal of Advanced Mechanical Design, Systems and Manufacturing* **7**, 422–431 (2013).

- <sup>17</sup>F. Ito, T. Kawaguchi, Y. Yamada, and T. Nakamura, “Development of a peristaltic-movement duct-cleaning robot for application to actual environment – examination of brush type and installation method to improve cleaning efficiency”, Journal of Robotics and Mechatronics **31**, 781–793 (2019).
- <sup>18</sup>A. A. Gargade and D. S. S. Ohol, “Development of In-pipe Inspection Robot”, IOSR Journal of Mechanical and Civil Engineering **13**, 64–72 (2016).
- <sup>19</sup>A. S. Boxerbaum, K. M. Shaw, H. J. Chiel, and R. D. Quinn, “Continuous wave peristaltic motion in a robot”, International Journal of Robotics Research **31**, 302–318 (2012).
- <sup>20</sup>J. Qiao, J. Shang, and A. Goldenberg, “Development of inchworm in-pipe robot based on self-locking mechanism”, IEEE/ASME Transactions on Mechatronics **18**, 799–806 (2013).
- <sup>21</sup>H.-J. Yeo, “Development of a Robot System for Repairing a Underground Pipe”, Journal of the Korea Academia-Industrial cooperation Society **13**, 1270–1274 (2012).
- <sup>22</sup>J. Y. Nagase, F. Fukunaga, and Y. Shigemoto, “Cylindrical elastic crawler mechanism for pipe inspection”, Advances in Cooperative Robotics: Proceedings of the 19th International Conference on Climbing and Walking Robots and the Support Technologies for Mobile Machines, CLAWAR 2016, 304–311 (2016).
- <sup>23</sup>*Standard test method for static and kinetic coefficients of friction of plastic film and sheeting*, <https://www.astm.org/Standards/D1894.htm>, [Online; accessed 11-March-2021].